

# CONTINUATION OF CONNECTING ORBITS IN 3D-ODES: (I) POINT-TO-CYCLE CONNECTIONS

E.J. DOEDEL<sup>1</sup>, B.W. KOOI<sup>2</sup>, YU.A. KUZNETSOV<sup>3</sup>, and G.A.K. van VOORN<sup>2</sup>

<sup>1</sup>*Department of Computer Science, Concordia University,  
1455 Boulevard de Maisonneuve O., Montreal, Quebec, H3G 1M8, Canada  
doedel@cs.concordia.ca*

<sup>2</sup>*Department of Theoretical Biology, Vrije Universiteit,  
de Boelelaan 1087, 1081 HV Amsterdam, the Netherlands  
kooi@bio.vu.nl, george.van.voorn@falw.vu.nl*

<sup>3</sup>*Department of Mathematics, Utrecht University  
Budapestlaan 6, 3584 CD Utrecht, the Netherlands  
kuznet@math.uu.nl*

February 1, 2008

## Abstract

We propose new methods for the numerical continuation of point-to-cycle connecting orbits in 3-dimensional autonomous ODE's using projection boundary conditions. In our approach, the projection boundary conditions near the cycle are formulated using an eigenfunction of the associated adjoint variational equation, avoiding costly and numerically unstable computations of the monodromy matrix. The equations for the eigenfunction are included in the defining boundary-value problem, allowing a straightforward implementation in AUTO, in which only the standard features of the software are employed. Homotopy methods to find connecting orbits are discussed in general and illustrated with several examples, including the Lorenz equations. Complete AUTO demos, which can be easily adapted to any autonomous 3-dimensional ODE system, are freely available.

*Keywords:* boundary value problems, projection boundary conditions, point-to-cycle connections, global bifurcations

# 1 Introduction

Many interesting phenomena in ODE systems can only be understood by analyzing global bifurcations. Examples of such are the occurrence and disappearance of chaotic behaviour. For example, the classical Lorenz attractor appears in a sequence of bifurcations, where *homoclinic orbits* connecting a saddle equilibrium to itself and *heteroclinic orbits* connecting an equilibrium point with a saddle cycle, are involved (Afraimovich et al., 1977). In the ecological context, Boer et al. (1999, 2001) showed that regions of chaotic behaviour in parameter space in some food chain models are bounded by bifurcations of point-to-cycle and cycle-to-cycle connections.

Thus, in order to gain more knowledge about the global bifurcation structure of a model, information is required on the existence of *homoclinic* and *heteroclinic* connections between equilibria and/or periodic cycles. The first type is a connection that links an equilibrium or a cycle to itself (asymptotically bi-stable, so it necessarily has nontrivial stable and unstable invariant manifolds). The second type is a connection that links an equilibrium or a cycle to another equilibrium or cycle.

The continuation of connecting orbits in ODE systems has been notoriously difficult. Doedel and Friedman (1989) and Beyn (1990) developed direct numerical methods for the computation of orbits connecting equilibrium points and their associated parameter values, based on truncated boundary value problems with *projection boundary conditions*. Moreover, Doedel, Friedman and Monteiro (1993) have proposed efficient methods to find starting solutions by successive continuations (homotopies). These continuation methods have been implemented in HOMCONT, as incorporated in AUTO (Doedel et al., 1997; Champneys and Kuznetsov, 1994; Champneys et al., 1996). HOMCONT is only suitable for the continuation of homoclinic point-to-point and heteroclinic point-to-point connections.

More recently, significant progress has been

made in the continuation of homoclinic and heteroclinic connections involving cycles. Dieci and Rebaza (2004) developed a method based on earlier works by Beyn (1994) and Pampel (2001). Their method is also based on projection boundary conditions, but uses an *ad hoc* multiple shooting technique and requires the numerical determination of the monodromy matrix associated with the periodic cycles involved in the connection.

In this paper, we propose new methods for the numerical continuation of point-to-cycle connections in 3-dimensional autonomous ODE's using projection boundary conditions. In our approach, the projection boundary conditions near each cycle are formulated using an eigenfunction of the associated adjoint variational equation, avoiding costly and numerically unstable computation of the monodromy matrix. Instead, the equations for the eigenfunction are included in the defining boundary-value problem, allowing a straightforward implementation in AUTO.

This paper is organized as follows. In Section 2 we recall basic properties of the projection boundary condition method to continue point-to-cycle connections. In Section 3 this method is adapted to efficient numerical implementation in a special – but important – 3D case. Homotopy methods to find connecting orbits are discussed in Section 4. Section 5 demonstrates that the algorithms allow for a straightforward implementation in AUTO, using only the basic features of this software. Three well-known examples (the three-dimensional Lorenz system, the electronic circuit model of Freire et al., 1993, and the standard three-level food chain model based on the Rosenzweig-MacArthur (1963) system) are used in Section 6 to illustrate the power of the new methods.

This is Part I of a sequel of two papers. Part II will deal with cycle-to-cycle connections in 3D systems.

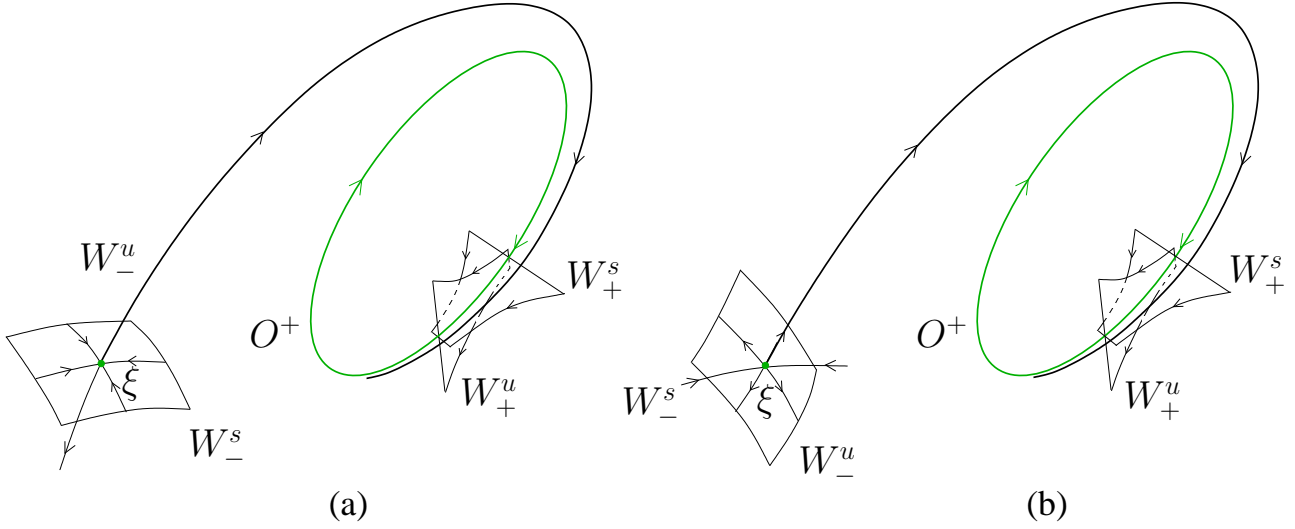


Figure 1: Point-to-cycle connecting orbits in  $\mathbb{R}^3$ : (a)  $n_u^- = 1$ ; (b)  $n_u^- = 2$ .

## 2 Truncated BVP's with projection BC's

Before presenting a BVP for a point-to-cycle connection, we set up some notation.

Consider a general system of ODE's

$$\frac{du}{dt} = f(u, \alpha), \quad (1)$$

where  $f : \mathbb{R}^n \times \mathbb{R}^p \rightarrow \mathbb{R}^n$  is a sufficiently smooth function of the state variables  $u \in \mathbb{R}^n$  and the control parameters  $\alpha \in \mathbb{R}^p$ . Denote by  $\varphi^t$  the (local) flow generated by (1)<sup>1</sup>.

Let  $O^-$  be either a saddle or a saddle-focus equilibrium, say  $\xi$ , and let  $O^+$  be a hyperbolic saddle limit cycle of (1). A solution  $u(t)$  of (1) defines a *connecting orbit* from  $O^-$  to  $O^+$  if

$$\lim_{t \rightarrow \pm\infty} \text{dist}(u(t), O^\pm) = 0 \quad (2)$$

(see Figure 1 for illustrations). Since  $u(t + \tau)$  satisfies (1) and (2) for any phase shift  $\tau$ , an additional scalar phase condition

$$\psi[u, \alpha] = 0 \quad (3)$$

<sup>1</sup>Whenever possible, we will not indicate explicitly the dependence of various objects on system parameters.

is needed to ensure uniqueness of the connecting orbit. This condition will be specified later.

For numerical approximation, the asymptotic conditions (2) are replaced by *projection boundary conditions* at the end-points of a large *truncation interval*  $[\tau_-, \tau_+]$ : The points  $u(\tau_-)$  and  $u(\tau_+)$  are required to belong to the linear subspaces that are tangent to the unstable and stable invariant manifolds of  $O^-$  and  $O^+$ , respectively.

Let  $n_u^-$  be the dimension of the unstable invariant manifold  $W_-^u$  of  $\xi$ , *i.e.*, the number of eigenvalues  $\lambda_u^-$  of the Jacobian matrix  $f_u = D_u f$  evaluated at the equilibrium which satisfy

$$\Re(\lambda^-) > 0.$$

Denote by  $x^+(t)$  a periodic solution (with minimal period  $T^+$ ) corresponding to  $O^+$  and introduce the *monodromy matrix*

$$M^+ = D_x \varphi^{T^+}(x) \Big|_{x=x^+(0)},$$

*i.e.*, the linearization matrix of the  $T^+$ -shift along orbits of (1) at point  $x_0^+ = x^+(0) \in O^+$ . Its eigenvalues  $\mu^+$  are called the *Floquet multipliers*; exactly one of them equals 1, due to the assumption of hyperbolicity. Let  $m_s^+ = n_s^+ + 1$  be the dimension of the stable invariant manifold  $W_+^s$  of the

cycle  $O^+$ ; here  $n_s^+$  is the number of its multipliers satisfying

$$|\mu^+| < 1.$$

A necessary condition to have an isolated *family* of point-to-cycle connecting orbits of (1) is that (see Beyn (1994))

$$p = n - m_s^+ - n_u^- + 2 \quad (4)$$

The projection boundary conditions in this case can be written as

$$L^-(u(\tau_-) - \xi) = 0, \quad (5a)$$

$$L^+(u(\tau_+) - x^+(0)) = 0, \quad (5b)$$

where  $L^-$  is a  $(n - n_u^-) \times n$  matrix whose rows form a basis in the orthogonal complement of the linear subspace that is tangent to  $W_-^u$  at  $\xi$ . Similarly,  $L^+$  is a  $(n - m_s^+) \times n$  matrix, such that its rows form a basis in the orthogonal complement to the linear subspace that is tangent to  $W_+^s$  of  $O^+$  at  $x^+(0)$ .

It can be proved that, generically, the truncated BVP composed of (1), a truncation of (3), and (5) has a unique solution family  $(\hat{u}, \hat{\alpha})$ , provided that (1) has a connecting solution family satisfying (3) and (4).

The truncation to the finite interval  $[\tau_-, \tau_+]$  implies an error. If  $u$  is a generic connecting solution to (1) at parameter value  $\alpha$ , then the following estimate holds:

$$\|(u|_{[\tau_-, \tau_+]}, \alpha) - (\hat{u}, \hat{\alpha})\| \leq C e^{-2 \min(\mu_- |\tau_-|, \mu_+ |\tau_+|)},$$

where  $\|\cdot\|$  is an appropriate norm in the space  $C^1([\tau_-, \tau_+], \mathbb{R}^n) \times \mathbb{R}^p$ ,  $u|_{[\tau_-, \tau_+]}$  is the restriction of  $u$  to the truncation interval, and  $\mu_{\pm}$  are determined by the eigenvalues of the Jacobian matrix and the monodromy matrix. See Pampel (2001) and Dieci and Rebaza (2004) for exact formulations, proofs, and references to earlier contributions.

### 3 New defining systems in $\mathbb{R}^3$

Here we explain how the projection boundary conditions (5) can be implemented efficiently in a

special – but important – case  $n = 3$ . Thereafter we specify the defining system used to continue connecting orbits in 3D-ODE example systems with AUTO. A saddle cycle  $O^+$  in such systems always has  $m_s^+ = m_u^+ = 2$ .

#### 3.1 The equilibrium-related part

The equilibrium point  $\xi$ , an appropriate solution of  $f(\xi, \alpha) = 0$ , cannot be found by time-integration methods because it is a saddle. There are two different types of saddle equilibria that can be connected to saddle cycles in 3D-ODE's. These are distinguished by the dimension  $n_u^-$  of the unstable invariant manifold  $W_-^u$  of  $\xi$ : We have either  $n_u^- = 1$  or  $n_u^- = 2$  (see Figure 1). In the former case, the connection is structurally unstable (has codim 1) and, according to (4), we need two free system parameters for its continuation ( $p = 2$ ). In the latter case, however, the connection is structurally stable and can be continued, generically, with one system parameter ( $p = 1$ ). There is a small difference in the implementation of the projection boundary condition (5a) in these two cases.

If  $n_u^- = 1$  (see Figure 2(a)), then the following *explicit projection boundary condition* replaces (5a):

$$u(\tau_-) = \xi + \varepsilon v, \quad (6)$$

where  $\varepsilon > 0$  is a given small number, and  $v \in \mathbb{R}^3$  is a unit vector that is tangent to  $W_-^u$  at  $\xi$ . Notice that this fixes the phase of the connecting solution  $u$ , so that (3) becomes (5a) in this case. The vector  $v$  in (6) is, of course, a normalized eigenvector associated with the unstable eigenvalue  $\lambda_u > 0$  of the Jacobian matrix  $f_u$  evaluated at the equilibrium. Hence, we can use the following algebraic system to continue  $\xi, v$  and  $\lambda_u$  simultaneously:

$$\begin{cases} f(\xi, \alpha) &= 0, \\ f_\xi(\xi, \alpha)v - \lambda_u v &= 0, \\ \langle v, v \rangle - 1 &= 0, \end{cases} \quad (7)$$

where  $\langle x, u \rangle = x^T u$  is the standard scalar product in  $\mathbb{R}^n$ .

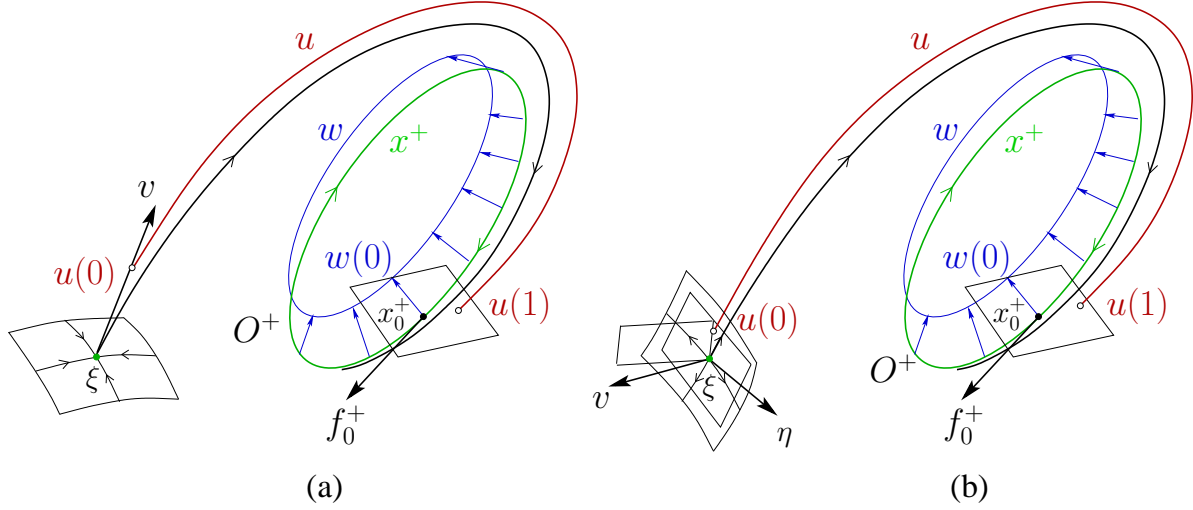


Figure 2: BVP's to approximate connecting orbits: (a)  $n_u^- = 1$ ; (b)  $n_u^- = 2$ .

If  $n_u^- = 2$  (see Figure 2(b)), then  $W_u^u$  is orthogonal to an eigenvector  $v$  of the *transposed* Jacobian matrix  $f_u^T$  corresponding to its eigenvalue  $\lambda_s < 0$ , so that (5a) can be written as

$$\langle v, u(\tau_-) - \xi \rangle = 0. \quad (8)$$

To continue  $\xi, v$ , and  $\lambda_s$ , we use a system similar to (7), namely:

$$\begin{cases} f(\xi, \alpha) = 0, \\ f_\xi^T(\xi, \alpha)v - \lambda_s v = 0, \\ \langle v, v \rangle - 1 = 0. \end{cases} \quad (9)$$

As a variant of the phase condition (3) in this case, we can use the linear condition

$$\langle \eta, u(\tau_-) - \xi \rangle = 0, \quad (10)$$

which places the starting point of the truncated connecting solution in a plane containing the equilibrium  $\xi$  and orthogonal to a fixed vector  $\eta$  (not collinear with  $v$ ).

### 3.2 The cycle and eigenfunctions

The heteroclinic connection is linked on the other side to a saddle limit cycle  $O^+$  (see Figure 2).

Thus, we also need a BVP to compute it. We use the standard periodic BVP:

$$\begin{cases} \dot{x}^+ - f(x^+, \alpha) = 0, \\ x^+(0) - x^+(T^+) = 0, \end{cases} \quad (11)$$

which is augmented by an appropriate phase condition that makes its solution unique. This phase condition is actually a boundary condition for the truncated connecting solution, and will be introduced below.

To set up the projection boundary condition for the truncated connecting solution  $u$  near  $O^+$ , we also need a vector, say  $w(0)$ , that is orthogonal at  $x(0)$  to the stable manifold  $W_+^s$  of the saddle limit cycle  $O^+$  (see Figure 2). It is well known that  $w(0)$  can be obtained from an *eigenfunction*  $w(t)$  of the *adjoint variational problem* associated with (11), corresponding to its eigenvalue

$$\mu = \frac{1}{\mu_u^+},$$

where  $\mu_u^+$  is a multiplier of the monodromy matrix  $M^+$  satisfying

$$|\mu_u^+| > 1$$

(see Appendix). The corresponding BVP is

$$\begin{cases} \dot{w} + f_u^T(x^+, \alpha)w = 0, \\ w(T^+) - \mu w(0) = 0, \\ \langle w(0), w(0) \rangle - 1 = 0, \end{cases} \quad (12)$$

where  $x^+$  is the solution of (11). In our implementation the above BVP is replaced by an equivalent BVP

$$\begin{cases} \dot{w} + f_u^T(x^+, \alpha)w + \lambda w &= 0, \\ w(T^+) - sw(0) &= 0, \\ \langle w(0), w(0) \rangle - 1 &= 0, \end{cases} \quad (13) \quad \text{as well as}$$

where  $s = \text{sign } \mu = \pm 1$  and

$$\lambda = \ln |\mu|$$

(see Appendix). In (13), the boundary conditions become periodic or anti-periodic, depending on the sign of the multiplier  $\mu$ , while the logarithm of its absolute value appears in the variational equation. This ensures high numerical robustness.

Given  $w$  satisfying (13), the projection boundary condition (5b) becomes

$$\langle w(0), u(\tau_+) - x^+(0) \rangle = 0. \quad (14)$$

### 3.3 The connection

Finally, we need a phase condition to select a unique periodic solution among those which satisfy (11), *i.e.*, to fix a *base point*  $x_0^+ = x^+(0)$  on the cycle  $O^+$  (see Figure 2). Usually, an integral condition is used to fix the phase of the periodic solution. For the point-to-cycle connection, however, we need a new condition, since the end point near the cycle should vary freely. To this end we require the end point of the connection to belong to a plane orthogonal to the vector  $f_0^+ = f(x^+(0), \alpha)$ . This gives the following BVP for the connecting solution:

$$\begin{cases} \dot{u} - f(u, \alpha) &= 0, \\ \langle f(x^+(0), \alpha), u(\tau_+) - x^+(0) \rangle &= 0. \end{cases} \quad (15)$$

### 3.4 The complete BVP

The complete truncated BVP to be solved numerically consists of (7), with

$$u(0) = \xi + \varepsilon v, \quad (16)$$

or (9), with

$$\langle v, u(0) - \xi \rangle = 0, \quad (17a)$$

$$\langle \eta, u(0) - \xi \rangle = 0, \quad (17b)$$

$$\dot{x}^+ - T^+ f(x^+, \alpha) = 0, \quad (18a)$$

$$x^+(0) - x^+(1) = 0, \quad (18b)$$

$$\langle w(0), u(1) - x^+(0) \rangle = 0, \quad (18c)$$

$$\dot{w} + T^+ f_u^T(x^+, \alpha)w + \lambda w = 0, \quad (18d)$$

$$w(1) - sw(0) = 0, \quad (18e)$$

$$\langle w(0), w(0) \rangle - 1 = 0, \quad (18f)$$

$$\dot{u} - T f(u, \alpha) = 0, \quad (18g)$$

$$\langle f(x^+(0), \alpha), u(1) - x^+(0) \rangle = 0. \quad (18h)$$

Here the time variable is scaled to the unit interval  $[0, 1]$ , so that both the cycle period  $T^+$  and the connecting time  $T$  become parameters.

If the connection time  $T$  is fixed at a large value, this BVP allows to continue simultaneously the equilibrium  $\xi$ , its eigenvalue  $\lambda_u$  or  $\lambda_s$ , the corresponding eigenvector  $v$ , the periodic solution  $x^+$  corresponding to the limit cycle  $O^+$ , its period  $T^+$ , the logarithm of the absolute value of the unstable multiplier of this cycle, the corresponding scaled eigenfunction  $w$ , as well as (a truncation of) the connecting orbit  $u$ . These objects become functions of one system parameter (when  $\dim W_-^u = 2$ ) or two system parameters (when  $\dim W_-^u = 1$ ). These free system parameters are denoted as  $\alpha_i$ .

If  $\dim W_-^u = 2$  then, generically, limit points (folds) are encountered along the solution family. These can be detected, located accurately, and subsequently continued in two system parameters, say,  $(\alpha_1, \alpha_2)$ , using the standard fold-following facilities of AUTO.

## 4 Starting strategies

The BVP's specified above can only be used if good starting data are available. This can be problematic, since global objects – a saddle cycle



and a connecting orbit – are involved. However, a series of successive continuations in AUTO can be used to generate all necessary starting data, given little *a priori* knowledge about the existence and location of a heteroclinic point-to-cycle connection.

## 4.1 The equilibrium and the cycle

The equilibrium  $\xi$ , its unstable or stable eigenvalue, as well as the corresponding eigenvector or adjoint eigenvector can be calculated using MAPLE or MATLAB. Alternatively, this saddle equilibrium can often be obtained via continuation of a stable equilibrium family through a limit point (fold) bifurcation.

To obtain the limit cycle  $O^+$ , one can continue numerically (with AUTO or CONTENT, for example) a limit cycle born at a Hopf bifurcation to an appropriate value of  $\alpha$ , from where we start the successive continuation.

## 4.2 Eigenfunctions

In the first of such continuations, the periodic solution corresponding the limit cycle at the particular parameter values is used to get an eigenfunction. To explain the idea, let us begin with the original adjoint eigenfunction  $w$ . Consider the periodic BVP (18a)–(18b) for the cycle, to which the standard integral phase condition is added,

$$\int_0^1 \langle \dot{x}_{old}^+(\tau), x^+(\tau) \rangle = 0, \quad (19)$$

as well as a BVP similar to (12), namely:

$$\begin{cases} \dot{w} + T^+ f_u^T(x^+, \alpha)w = 0, \\ w(1) - \mu w(0) = 0, \\ \langle w(0), w(0) \rangle - h = 0. \end{cases} \quad (20)$$

In (19),  $x_{old}^+$  is a reference periodic solution, typically the one in the preceding continuation step. The parameter  $h$  in (20) is a *homotopy parameter*, that is set to zero initially. Then (20) has a trivial solution

$$w(t) \equiv 0, \quad h = 0,$$

for any real  $\mu$ . This family of trivial solutions parametrized by  $\mu$  can be continued in AUTO using a BVP consisting of (11) (with scaled time variable  $t$ ), (19), and (20) with free parameters  $(\mu, h)$  and fixed  $\alpha$ . A Floquet multiplier of the adjoint system then corresponds to a branch point at  $\mu_1$  along this trivial solution family (see Appendix). AUTO can accurately locate such a point and switch to the nontrivial branch that emanates from it. Continuing this secondary family in  $(\mu, h)$  until, say, the value  $h = 1$  is reached, gives a nontrivial eigenfunction  $w$  corresponding to the multiplier  $\mu_1$ . Note that in this continuation the value of  $\mu$  remains constant,  $\mu \equiv \mu_1$ , up to numerical accuracy.

The same method is applicable to obtain a nontrivial scaled adjoint eigenfunction. For this, the BVP

$$\begin{cases} \dot{w} + T^+ f_u^T(x^+, \alpha)w + \lambda w = 0, \\ w(1) - s w(0) = 0, \\ \langle w(0), w(0) \rangle - h = 0, \end{cases} \quad (21)$$

where  $s = \text{sign}(\mu)$ , replaces (20). A branch point at  $\lambda_1$  then corresponds to the adjoint multiplier  $se^{\lambda_1}$ . Branch switching then gives the desired eigendata.

## 4.3 The connection

Sometimes, an approximation of the connecting orbit can be obtained by time-integration of (1) with a starting point satisfying (6) or (8) and (10). These data (the periodic solution corresponding to the limit cycle, its nontrivial eigenfunction, and the integrated connecting orbit) must then be merged, using the same scaled time variable and mesh points. This only works for non-stiff systems provided that the connecting orbit and its corresponding parameter values are known *a priori* with high accuracy, which is not the case for most models.

A practical remedy in most cases is to apply the method of *successive continuation* first introduced by Doedel, Friedman and Monteiro (1993) for point-to-point problems. This method does

not guarantee that a connection will be found but works well if we start sufficiently close to a connection *in the parameter space*. Here we generalize this method to point-to-cycle connections.

We first consider the case  $\dim W_-^u = 1$ . To start, we introduce a BVP composed of (7), (16), and a modified version of (18), namely:

$$\dot{x}^+ - T^+ f(x^+, \alpha) = 0, \quad (22a)$$

$$x^+(0) - x^+(1) = 0, \quad (22b)$$

$$\Psi[x^+] = 0, \quad (22c)$$

$$\dot{w} + T^+ f_u^T(x^+, \alpha)w + \lambda w = 0, \quad (22d)$$

$$w(1) - sw(0) = 0, \quad (22e)$$

$$\langle w(0), w(0) \rangle - 1 = 0, \quad (22f)$$

$$\dot{u} - Tf(u, \alpha) = 0, \quad (22g)$$

$$\langle f(x^+(0), \alpha), u(1) - x^+(0) \rangle - h_1 = 0, \quad (22h)$$

where  $\Psi$  in (22c) defines any phase condition fixing the base point  $x^+(0)$  on the cycle  $O^+$ ; for example

$$\Psi[x^+] = x_j^+(0) - a_j,$$

where  $a_j$  is the  $j$ th-coordinate of the base point at some given parameter values, and  $h_1$  is a *homotopy parameter*.

Take an initial solution to this BVP that collects the previously found equilibrium-related data, the cycle-related data  $(x^+, T^+)$  including  $x^+(0)$ , the eigenfunction-related data  $(w, \lambda)$ , as well as the value of  $h_1$  computed for the initial “connection”

$$u(\tau) = \xi + \varepsilon v e^{\lambda_u T \tau}, \quad \tau \in [0, 1], \quad (23)$$

which is a solution of the scaled linear approximation of (1) in the tangent line to the unstable manifold  $W_-^u$  of  $\xi$ . By continuation in  $(T, h_1)$  for a fixed value of  $\alpha$ , we try to make  $h_1 = 0$ , while  $u(1)$  is near the cycle  $O^+$ , so that  $T$  becomes sufficiently large.

After this is accomplished, we introduce another BVP composed of (7), (16), and

$$\dot{x}^+ - T^+ f(x^+, \alpha) = 0, \quad (24a)$$

$$x^+(0) - x^+(1) = 0, \quad (24b)$$

$$\langle w(0), u(1) - x^+(0) \rangle - h_2 = 0, \quad (24c)$$

$$\dot{w} + T^+ f_u^T(x^+, \alpha)w + \lambda w = 0, \quad (24d)$$

$$w(1) - sw(0) = 0, \quad (24e)$$

$$\langle w(0), w(0) \rangle - 1 = 0, \quad (24f)$$

$$\dot{u} - Tf(u, \alpha) = 0, \quad (24g)$$

$$\langle f(x^+(0), \alpha), u(1) - x^+(0) \rangle = 0, \quad (24h)$$

where  $h_2$  is another homotopy parameter.

Using the solution obtained in the previous step, we can activate one of the system parameters, say  $\alpha_1$ , and aim to find a solution with  $h_2 = 0$  by continuation in  $(\alpha_1, h_2)$  for fixed  $T$ . Then we can improve the connection by continuation in  $(\alpha_1, T)$ , restarting from this latest solution, in the direction of increasing  $T$ . Eventually, we fix a sufficiently large value of  $T$  and continue the (approximate) connecting orbit in two systems parameters, say  $(\alpha_1, \alpha_2)$ , using the original BVP without any homotopy parameter as described in Section 3.4. All these steps are illustrated for the Lorenz example in Section 6.1. In practice, intermediate continuations in  $\varepsilon$  or other system parameters may be necessary to obtain a good approximation to the connecting orbit.

When  $\dim W_-^u = 2$ , a minor modification of the above homotopy method is required. In this case, we replace (17) by the explicit boundary conditions

$$u(0) - \xi - \varepsilon(c_1 v^{(1)} + c_2 v^{(2)}) = 0, \quad (25a)$$

$$c_1^2 + c_2^2 = 1, \quad (25b)$$

where  $\varepsilon$  is a small parameter specifying the distance between  $u(0)$  and  $\xi$ ,  $v^{(j)}$  are two linear-independent vectors tangent to  $W_-^u$  of the saddle  $\xi$ , and  $c_{1,2}$  are two new scalar homotopy parameters. Note that if  $v = (v_1, v_2, v_3)^T$  is a solution to (9) with  $v_2 \neq 0$ , then one can use the normalized vectors

$$v^{(1)} = \begin{pmatrix} v_2 \\ -v_1 \\ 0 \end{pmatrix}, \quad v^{(2)} = \begin{pmatrix} 0 \\ v_3 \\ -v_2 \end{pmatrix}.$$



Now consider a BVP composed of (9), (25), and (22). The initial data for this BVP are the same as in the case  $\dim W_-^u = 1$ , except for

$$c_1 = 1, \quad c_2 = 0.$$

The initial “connection” in this case is

$$u(\tau) = \xi + \varepsilon e^{\tau T A} v^{(1)}, \quad \tau \in [0, 1], \quad (26)$$

where  $A = f_u(\xi, \alpha)$ , to be used to compute the initial value of  $h_1$  in (22h).

By continuation in  $(T, h_1)$  (and, eventually, in  $(c_1, c_2, h_1)$ ) for fixed values of all other parameters, we aim to locate a solution with  $h_1 = 0$ , with  $u(1)$  near the base point of the cycle  $O^+$ , so that  $T$  becomes sufficiently large. We then switch to the BVP composed of (7), (25), and (24), and we aim to locate a solution with  $h_2 = 0$ , by continuation in  $(c_1, c_2, h_2)$  for fixed  $T$ . When this is achieved, we have a solution to the original BVP (9), (17), and (18) introduced in Section 3.4 and containing no homotopy parameters. Using this BVP, we can continue the approximate connecting orbit in one system parameter, say  $\alpha_1$ , with  $T$  fixed.

Examples of such successive continuations will be given in Section 6.3, where we consider the standard model of a 3-level food chain. In that section also an alternative BVP formulation for (25) is given. When one system parameter is varied, limit points (folds) can be found and then continued in two system parameters.

## 5 Implementation in AUTO

Our algorithms have been implemented in AUTO, which solves the boundary value problems using superconvergent *orthogonal collocation* with adaptive meshes. AUTO can compute paths of solutions to boundary value problems with integral constraints and non-separated boundary condi-

tions:

$$\dot{U}(\tau) - F(U(\tau), \beta) = 0, \quad \tau \in [0, 1], \quad (27a)$$

$$b(U(0), U(1), \beta) = 0, \quad (27b)$$

$$\int_0^1 q(U(\tau), \beta) d\tau = 0, \quad (27c)$$

where

$$U(\cdot), F(\cdot, \cdot) \in \mathbb{R}^{n_d}, \quad b(\cdot, \cdot) \in \mathbb{R}^{n_{bc}}, \quad q(\cdot, \cdot) \in \mathbb{R}^{n_{ic}},$$

and

$$\beta \in \mathbb{R}^{n_{fp}}.$$

Here  $\beta$  represents the  $n_{fp}$  *free parameters* that are allowed to vary, where

$$n_{fp} = n_{bc} + n_{ic} - n_d + 1. \quad (28)$$

The function  $q$  can also depend on  $\dot{U}$  and on the derivative of  $U$  with respect to pseudo-arclength, as well as on  $\hat{U}$ , the value of  $U$  at the previously computed point on the solution family.

For our primary BVP problem (7) or (9) with (16) or (17), respectively, and (18), we have

$$n_d = 9, \quad n_{ic} = 0,$$

and  $n_{bc} = 19$  or  $18$ , respectively, since (7) and (9) are treated as boundary conditions.

## 6 Examples

In this section we illustrate the performance of our algorithm by applying it to three model systems, namely, the Lorenz equations, an electronic circuit model, and a biologically relevant system.

### 6.1 The Lorenz system

One of the best-known dynamical systems that has a heteroclinic point-to-cycle connection is the three-dimensional Lorenz system, given by

$$\begin{cases} \dot{x}_1 &= \sigma(x_2 - x_1), \\ \dot{x}_2 &= rx_1 - x_2 - x_1x_3, \\ \dot{x}_3 &= x_1x_2 - bx_3, \end{cases} \quad (29)$$

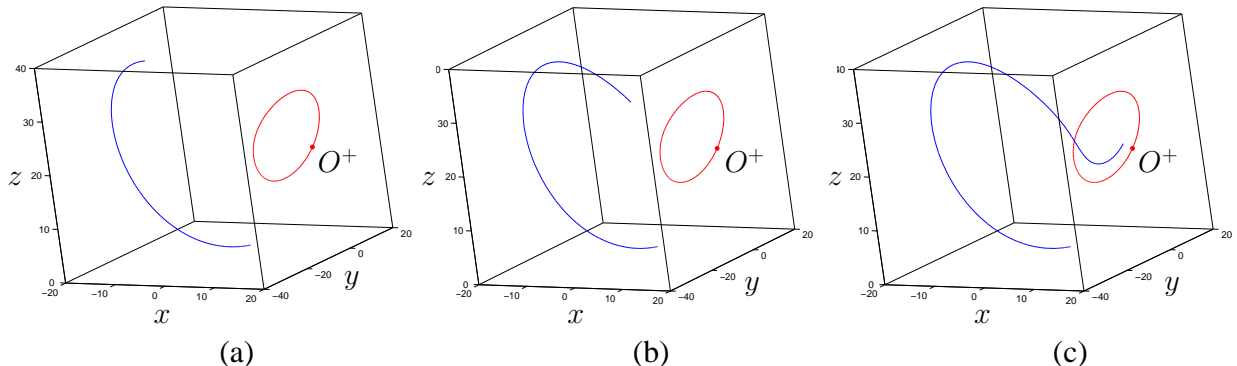


Figure 3: Continuation in  $T$ : (a)  $T = 1.43924$ ; (b)  $T = 1.54543$ ; (c)  $T = 2.00352$ .

with standard parameter values  $\sigma = 10$ ,  $b = 8/3$ , and where  $r$  is the usual bifurcation parameter. With these parameter values, a supercritical pitchfork bifurcation from the trivial equilibrium occurs at  $r = 1$ , giving rise to two symmetric nontrivial equilibria. At  $r \approx 13.962$  there are two symmetry-related orbits of infinite period that are homoclinic to the origin, and from which two families of saddle cycles arise (together with a nontrivial hyperbolic invariant set). A subcritical Hopf bifurcation of nontrivial equilibria takes place at  $r_H \approx 24.7368$ , where these two cycles disappear.

At a critical value  $r_{het}$  there is a heteroclinic point-to-cycle connection, that generates a chaotic attractor, see Afraimovich et al. (1977). Its domain of attraction is bounded by the stable invariant manifolds of the saddle cycles. Beyn (1990) found  $r_{het} \approx 24.05$ , and later Dieci and Rebaza (2004) calculated

$$r_{het} = 24.057900322267 \dots$$

The heteroclinic connection can be continued in two parameters, for example  $r$  and  $\sigma$  with  $b$  fixed. The resulting curve in the  $r, \sigma$ -plane was first shown in Appendix II, written by L.P. Shil'nikov, to the Russian translation of the book by Marsden and McCracken (see Pampel (2001), Dieci and Rebaza (2004), for more recent related results). As shown by Bykov and Shilnikov (1992),

the canonical Lorenz attractor appears by crossing only a part of the heteroclinic connection curve.

We begin at  $r = 21.0$  and consider a saddle limit cycle  $O^+$  of (29) with the base point

$$x^+(0) = (9.265335, 13.196014, 15.997250)$$

and period  $T^+ = 0.816222$ . This cycle can be obtained easily by continuation in AUTO and has two nontrivial multipliers:

$$\mu_s^+ = 0.0000113431, \quad \mu_u^+ = 1.26094.$$

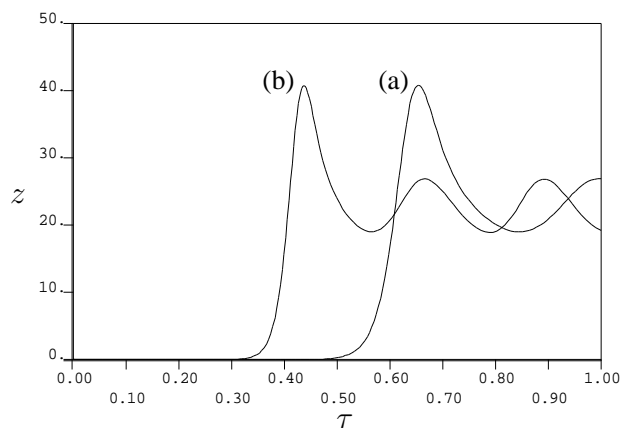


Figure 4: Two profiles of the truncated connecting orbit in the Lorenz system scaled to the unit time interval: (a)  $T = 2.00352$ ; (b)  $T = 3.0$ .

To compute the eigenfunction  $w$ , we first continue the trivial solution of the BVP (18a), (18b),

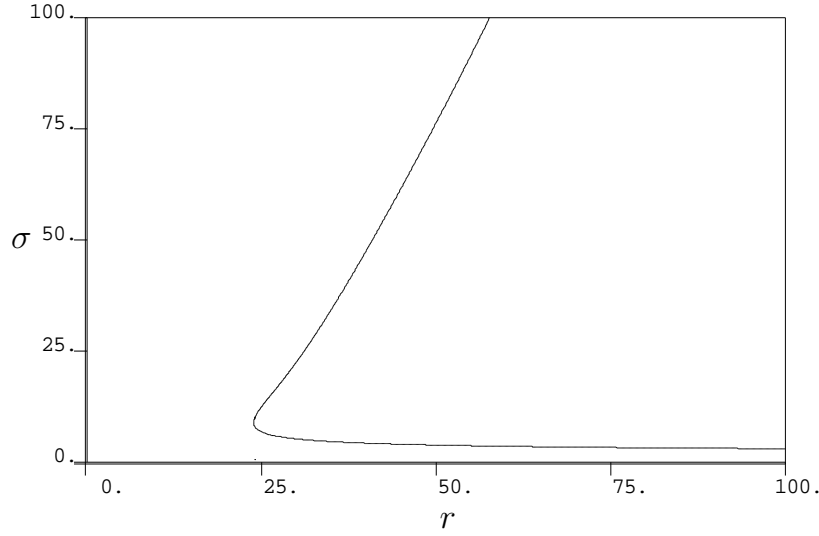


Figure 5: The bifurcation curve of the Lorenz system corresponding to the point-to-cycle connection.

(19), and (21), to detect a branch point at

$$\lambda = \ln(\mu_u^+) = 0.231854,$$

from which a nontrivial branch is followed until the value  $h = 1$  is reached. This gives a nontrivial eigenfunction  $w(t)$ , with  $\|w(0)\| = 1$ , namely,

$$w(0) = (0.168148, 0.877764, -0.448616)^T.$$

In these continuations all problem parameters, that is  $r, \sigma$ , and  $b$ , are fixed.

The next step is to find an approximation to the connecting orbit. For this, we consider the BVP (7), (16), and (22) with

$$\Psi[x^+] = x_1^+(0) - 9.265335$$

and continue its solution at fixed system parameters with respect to  $(T, h_1)$ . Figure 3 shows three consecutive solutions with  $h_1 = 0$ . The end point of the last solution (with  $T = 2.00352$ ) is located near the base point  $x^+(0)$  of the cycle  $O^+$ . Using this solution as the initial data for the BVP (7), (16), and (24), we do a continuation in  $(r, h_2)$  with  $T$  fixed until  $h_2 = 0$  is detected. This occurs at  $r = 24.0720$ , and ensures that the end point of the connection is in a plane orthogonal to  $w(0)$ , *i.e.*, in the tangent plane to  $W_+^s$  at  $x^+(0)$ .

The primary BVP consisting of (7), (16), and (18) is used for further continuation runs. First, the length of the connecting orbit is increased by continuation in  $(r, T)$  until  $T = 3.0$ . The corresponding parameter value  $r = 24.0579$  gives a good approximation for  $r_{het}$ , since the ‘tail’ of the connecting orbit follows the cycle  $O^+$  several times; (see Figure 4).

Finally, continuation in the two system parameters  $(r, \sigma)$  with  $T$  fixed, gives the bifurcation curve corresponding to the point-to-cycle connection in (29), see Figure 5.

## 6.2 A circuit model

The next example is one from the HOMCONT demos of Champneys *et al.* (1999), namely, the electronic circuit model of Freire *et al.* (1993; see also the AUTO demos *tor* and *cir*). The equations are

$$\begin{cases} r\dot{x}_1 &= -(\beta + \nu)x_1 + \beta x_2 - a_3 x_1^3 + b_3(x_2 - x_1)^3, \\ \dot{x}_2 &= \beta x_1 - (\beta + \gamma)x_2 - x_3 - b_3(x_2 - x_1)^3, \\ \dot{x}_3 &= x_2, \end{cases} \quad (30)$$

where  $\gamma = 0$ ,  $r = 0.6$ ,  $a_3 = 0.328578$ ,  $b_3 = 0.933578$ , and  $\nu$  and  $\beta$  are bifurcation parameters. With HOMCONT it was shown previously that a homo-

clinic connection to the origin occurs for

$$\nu_{init} = -0.721309, \beta_{init} = 0.6$$

with truncated time interval  $T = 200$ . Continuation in two-parameter dimension then leads to a Shil'nikov-Hopf bifurcation at

$$\nu = -1.026445, \beta = -2.330391 \cdot 10^{-5},$$

where a limit cycle bifurcates from the equilibrium, effectively turning the homoclinic connection into a heteroclinic one (see AUTO demo *cir*). We can now compare the results from the continuation in HOMCONT with the results from the application of our BVP system.

The equilibrium in this system is a saddle-focus, and we therefore have  $n_s^- = 2$  and  $n_u^- = 1$ . To generate appropriate starting data we locate a Hopf bifurcation, with  $\beta$  as free parameter, from where a cycle is continued up to a selected value of  $\beta$ , say,  $\beta = -0.32$ . The saddle limit cycle  $O^+$  has the base point

$$x^+(0) = (0.03448278, 0.46460323, 0.4737975)$$

and period  $T^+ = 6.3646138$ . The nontrivial multipliers are

$$\mu_s^+ = 3.986051 \cdot 10^{-6}, \mu_u^+ = 18.85438$$

The eigenfunction of this cycle is computed as described in Section 4.2, which yields

$$w(0) = (0.99950, -0.019205, 0.024767)^T$$

and the log multiplier

$$\lambda = -13.579343187.$$

An approximation of the connecting orbit is then obtained using BVP (7), (16), and (22), with

$$\Psi[x^+] = x_2^+(0) - 0.46460323.$$

The software CONTENT is used to get a good approximation of the connection period  $T$ , after which shooting in MATLAB is used to obtain the orbit itself for the given period.

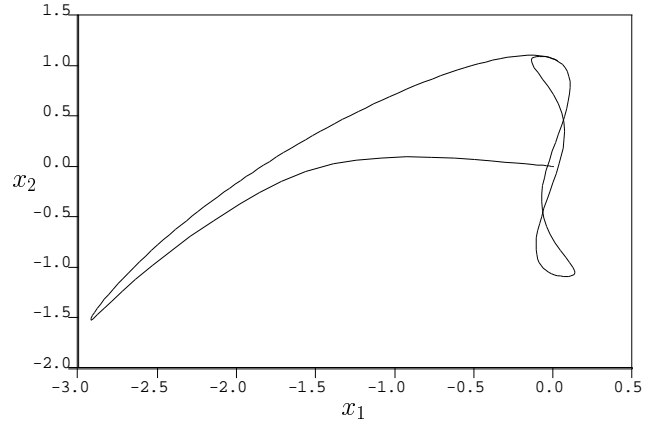


Figure 6: A point-to-cycle connection of the electronic circuit model, projected onto the  $x_1, x_2$ -plane.

Continuation of this approximate orbit with respect to  $(T, h_1)$  yields several orbits with  $h_1 = 0$ . For  $T = 11.59816$  the orbit is close enough to the  $x_2$  base coordinate to use the data for the BVP (7), (16), and (24). Continuation in  $(\nu, h_2)$  is done until a zero of  $h_2$  is reached.

The primary BVP (7), (16), and (18) is used in the subsequent computations. Continuation in  $(\nu, T)$  gives orbits of any desired period  $T$ ; we used  $T = 20$  with

$$\nu = -1.500498.$$

At this point continuation can be done in  $(\nu, \beta)$ .

In Figure 6 we see a point-to-cycle connection in a  $x_1, x_2$ -plot at some selected parameter values. It is apparent that the homotopy method has resulted in a good approximation of the connecting orbit. Figure 7 shows the composite results of the two-parameter continuation of the homoclinic connection in HOMCONT and our continuation of the heteroclinic connection. Label 5 is the starting point of the continuation of the homoclinic connection that terminates at the solution labelled 1. Beyond this solution HOMCONT gives spurious results. Note that label 1 coincides with label 9, where the curve of the heteroclinic connection turns back onto itself, *i.e.*, the continuation reverses direction approximately at the

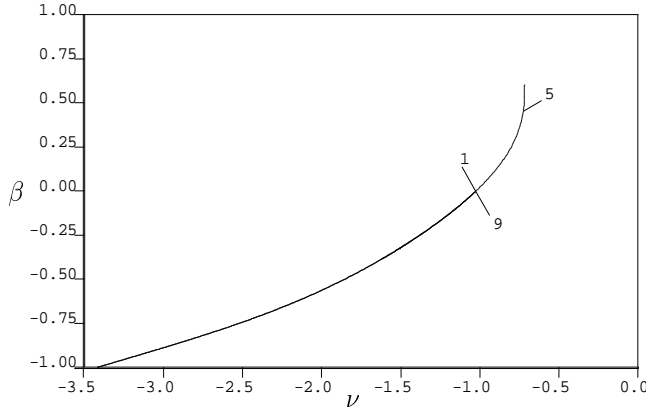


Figure 7: Continuation in  $(\nu, \beta)$  of the point-to-cycle connection, as explained in detail in the text.

point where the Shil'nikov-Hopf bifurcation occurs. Plots in AUTO of the limit cycle data (not shown) reveal that indeed the cycle shrinks practically to a point, before the continuation reverses direction.

### 6.3 A food chain model

The following three-level food chain model from theoretical biology is based on the Rosenzweig-MacArthur (1963) prey-predator model. The equations are given by

$$\begin{cases} \dot{x}_1 &= x_1(1 - x_1) - f_1(x_1, x_2), \\ \dot{x}_2 &= f_1(x_1, x_2) - f_2(x_2, x_3) - d_1 x_2, \\ \dot{x}_3 &= f_2(x_2, x_3) - d_2 x_3, \end{cases} \quad (31)$$

with Holling Type-II functional responses

$$f_i(u, v) = \frac{a_i uv}{1 + b_i u}, \quad i = 1, 2.$$

The death rates  $d_1$  and  $d_2$  are used as bifurcation parameters, with the other parameters set at  $a_1 = 5$ ,  $a_2 = 0.1$ ,  $b_1 = 3$ , and  $b_2 = 2$ .

It is well known that this model displays chaotic behaviour in a given parameter range, see Hogue and Hesper (1978), Klebanoff and Hastings (1994), McCann and Yodzis (1995), Kuznetsov and Rinaldi (1996), and Kuznetsov et al. (2001).

Previous work by Boer et al. (1999, 2001) has also shown that the regions of chaos are intersected by homoclinic and heteroclinic global connections. In particular, a heteroclinic point-to-cycle orbit connecting a saddle with a two-dimensional unstable manifold to a saddle cycle with a two-dimensional stable manifold can exist. It was shown that the stable manifold of this limit cycle forms the basin boundary of the interior attractor and that the boundary has a complicated structure, especially near the equilibrium, when the heteroclinic orbit is present. These and other results were obtained numerically using multiple shooting. In this section we reproduce these results for the heteroclinic point-to-cycle connection. Using our homotopy method we obtain an accurate approximation of the heteroclinic orbit. A one-parameter bifurcation diagram then shows limit points, which correspond to tangencies of the above-mentioned two-dimensional manifolds. We then continue the limit points in two parameters.

A starting point can be found, for example, at  $d_1 \approx 0.2080452$ ,  $d_2 = 0.0125$ , where there is a fold bifurcation in which two limit cycles appear. This also corresponds to the birth of the heteroclinic point-to-cycle connection.

Before using the homotopy method to obtain an approximation of the point-to-cycle connection, we locate a Hopf bifurcation, for instance at  $d_1 \approx 0.51227$ ,  $d_2 = 0.0125$ . The limit cycle born at this Hopf bifurcation is continued up to a selected value of  $d_1$ , say,  $d_1 = 0.25$ .

We now have an equilibrium

$$\xi = (0.74158162, 0.16666666, 11.997732)$$

and a saddle limit cycle with the base point

$$x^+(0) = (0.839705, 0.125349, 10.55289)$$

and period  $T^+ = 24.282248$ . Its nontrivial multipliers are

$$\mu_s^+ = 0.6440615, \mu_u^+ = 6.107464 \cdot 10^2.$$

The eigenfunction  $w$  is obtained as described in the previous sections. Continuation of the trivial solution of the BVP (18a), (18b), (19), and

(21) and the subsequent continuation of the bifurcating family until  $h = 1$ , yields the multiplier

$$\lambda = \ln(\mu_s^+) = -0.439961.$$

Note that we use the stable multiplier, because of the projection boundary conditions. The associated nontrivial eigenfunction  $w(t)$  with  $\|w(0)\| = 1$  has

$$w(0) = (0.09306, -0.87791, -4.69689)^T.$$

We now consider a BVP composed of (9), (25a), and (22). Using CONTENT and MATLAB we obtain an approximation of the connection with the boundary condition

$$\Psi[x^+] = x_2^+(0) - 0.125349$$

and period  $T = 155.905$ . The starting point is calculated by splitting the normalized adjoint stable vector (evaluated at  $d_1 = 0.25, d_2 = 0.0125$ )

$$v = (0.098440, 0.168771, 0.0049532)^T$$

into  $v^{(1)}$  and  $v^{(2)}$ , as described in Section 4.3, and multiplying it by a small  $\varepsilon$ , say  $\varepsilon = 0.001$ . In our case the starting point was

$$u(0) = (0.742445, 0.166163, 11.997732).$$

The first homotopy step involves continuation in  $(h_1, T)$ . However, this does not lead to zeroes of  $h_1$ . To obtain  $h_1 = 0$  we expand the previous set of BVPs with (25b). Subsequent continuation in  $(c_1, c_2, h_1)$  gives a solution with  $h_1 = 0$  that indeed ends near the base point  $x^+(0)$  of the limit cycle.

For continuation in the second homotopy step, a switch is made to a BVP composed of (9), (24) and (25). Continuation in  $(c_1, c_2, h_2)$  leads to some solutions with  $h_2 = 0$ .

The obtained approximate connecting point-to-cycle connection now suffices for continuation in system parameters. Before doing a continuation in a system parameter the connection is improved by increasing the connection period. A user-defined point of  $T = 300$  suffices. Next,

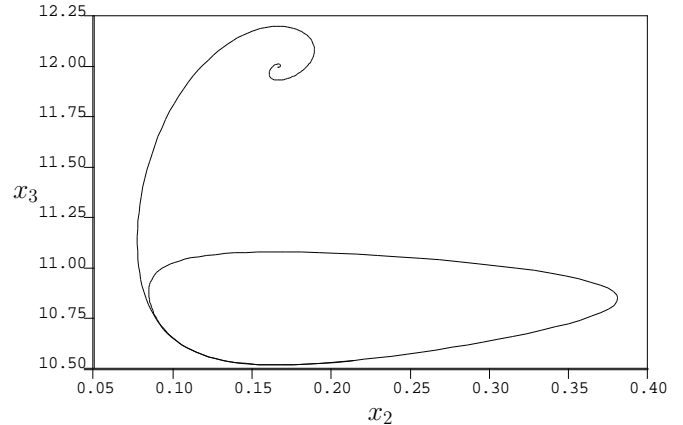


Figure 8: An approximation to the point-to-cycle connection projected onto the  $(x_2, x_3)$ -plane for the food chain model with  $a_1 = 5$ ,  $a_2 = 0.1$ ,  $b_1 = 3$ ,  $b_2 = 2$ ,  $d_1 = 0.25$ , and  $d_2 = 0.0125$ .

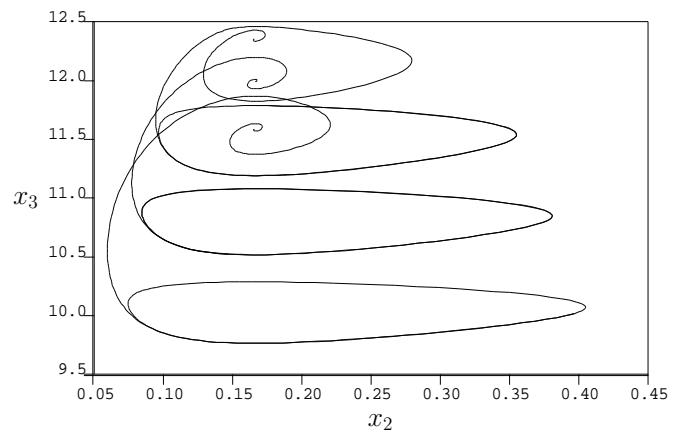


Figure 9: Several point-to-cycle connections in the food chain model with different values of  $d_1$ .



the parameter  $\varepsilon$  is decreased up to a user-defined point of  $\varepsilon = -1 \cdot 10^{-5}$ , so that the starting point  $u(0)$  is slightly away from the equilibrium  $\xi$ . Figure 8 displays a projection of the point-to-cycle connection onto the  $(x_2, x_3)$ -plane.

Now the connecting orbit can be continued up to a limit point in one system parameter. Figure 9 displays three connecting orbits obtained after continuation with respect to  $\alpha_1 = d_1$ . Continuations in  $d_1$  result in the detection of the points

$$d_1 = 0.280913 \quad \text{and} \quad d_1 = 0.208045$$

where the first one is a limit point and the second one a termination point. This point coincides with a tangent bifurcation for the limit cycle to which the point-to-cycle orbit connects. Continuations in  $d_2$  result in the detection of the points

$$d_2 = 0.0130272 \quad \text{and} \quad d_2 = 9.51660 \cdot 10^{-3}$$

which are both limit points. Any of the detected limit points can now be used as a starting point for a two-parameter continuation in  $\alpha = d_1$  or  $d_2$ . In practice, the connection period may have to be increased or decreased to obtain the full two-parameter continuation curve. In the demo, the last limit point ( $d_2 = 9.51660 \cdot 10^{-3}$ ) is the one selected for the food chain model. The two-parameter continuation curve terminates at both ends in codim 2 points lying on the above-mentioned tangent bifurcation for the limit cycle. These points coincide with the log multiplier  $\lambda = 0$ . Observe that this corresponds to the point  $d_1 = 0.208045$ , detected in the one-parameter continuation, where also  $\lambda = 0$ .

For the continuation in two system parameters, the BC (25) proves ineffective, since it leads to the detection of several spurious limit points. This is, because the orbit spiralling out from the equilibrium has an elliptical shape. The circle of a small radius, centered at the equilibrium, intersects the spiral at several points, one of which is the starting point of the connecting orbit. During continuation, with a changing problem parameter, the spiral will change size and the starting

point on the circle may collide with another such point where the circle and the spiral intersect. This intersection would correspond to a fold with respect to the problem parameter. As a result, to obtain a full continuation curve of the connecting orbit in two system parameters, some restarts are required.

In order to avoid these spurious folds, we returned to the original BC (17) with (17b) in the form

$$u_j(0) - \xi_j = 0, \quad (32)$$

where  $j$  is either 1, 2 or 3. By setting  $j = 2$  we are in line with the work by Boer et al. (2001), who used a Poincaré plane through the equilibrium  $\xi$  where  $x_2 = \xi_2$ .

Figure 10 shows the curve of limit points  $T_{het}$  that is computed with the method described above, using the standard switching and fold-following facilities of AUTO. This curve can be obtained in one run, given the connection period is chosen conveniently. It agrees with the results previously obtained by Boer et al. (1999) by labourious multiple shooting.

## 7 Discussion

Our continuation method for point-to-cycle connections, using homotopies in a boundary value setting is both robust and time-efficient. Detailed AUTO demos that carry out the computations described in Section 6 are freely downloadable from [www.bio.vu.nl/thb/research/project/globif](http://www.bio.vu.nl/thb/research/project/globif).

Although the method was presented for 3D-systems, it can be extended directly to point-to-cycle connections in  $n$ -dimensional systems, when the unstable invariant manifold of the equilibrium  $\xi$  is either one-dimensional or has codimension one, while the stable invariant manifold of the cycle  $O^+$  has codimension one.

In the forthcoming Part II of this paper, we will extend our method to include detection and continuation of cycle-to-cycle connections.

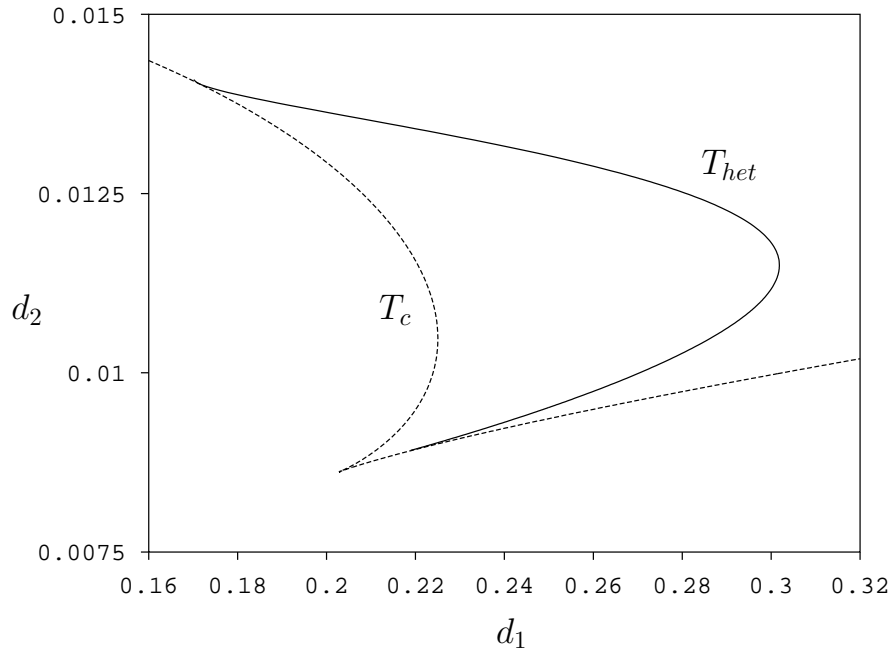


Figure 10: A two-parameter bifurcation diagram of the food chain model that shows the region where there exist point-to-cycle connections. The region is bounded on one side by the cycle fold, ( $T_c$ ), and on the other side by the curve  $T_{het}$ , the locus of limit points of the heteroclinic connections.

## References

- [Afraimovich *et al.*, 1977] V. S. Afraimovich, V. V. Bykov, and L. P. Shilnikov, [1977], “The origin and structure of the Lorenz attractor,” *Dokl. Akad. Nauk SSSR*, **234**, 336–339.
- [Beyn, 1990] W.-J. Beyn, [1990], “The numerical computation of connecting orbits in dynamical systems,” *IMA J. Numer. Anal.*, **10**, 379–405.
- [Beyn, 1994] W.-J. Beyn, [1994], “On well-posed problems for connecting orbits in dynamical systems.”, In *Chaotic Numerics (Geelong, 1993)*, volume 172 of *Contemp. Math.*, 131–168. Amer. Math. Soc., Providence, RI.
- [Boer *et al.*, 1999] M. P. Boer, B. W. Kooi, and S. A. L. M. Kooijman, [1999], “Homoclinic and heteroclinic orbits to a cycle in a tri-trophic food chain,” *J. Math. Biol.*, **39**, 19–38.
- [Boer *et al.*, 2001] M. P. Boer, B. W. Kooi, and S. A. L. M. Kooijman, [2001], “Multiple attractors and boundary crises in a tri-trophic food chain,” *Math. Biosci.*, **169**, 109–128.
- [Bykov and Shilnikov, 1992] V. V. Bykov and A. L. Shilnikov, [1992], “On the boundaries of the domain of existence of the Lorenz attractor,” *Selecta Mathematica Sovietica*, **11**, 375–382.
- [Champneys and Kuznetsov, 1994] A. R. Champneys and Yu. A. Kuznetsov, [1994], “Numerical detection and continuation of codimension-two homoclinic bifurcations,” *Internat. J. Bifur. Chaos Appl. Sci. Engrg.*, **4**, 785–822.
- [Champneys *et al.*, 1996] A. R. Champneys, Yu. A. Kuznetsov, and B. Sandstede, [1996], “A numerical toolbox for homoclinic bifurcation analysis,” *Internat. J. Bifur. Chaos Appl. Sci. Engrg.*, **6**, 867–887.
- [Dieci and Rebaza, 2004a] L. Dieci and J. Rebaza, [2004], “Erratum: “Point-to-periodic and periodic-to-periodic connections,”” *BIT Numerical Mathematics*, **44**, 617–618.
- [Dieci and Rebaza, 2004b] L. Dieci and J. Rebaza, [2004], “Point-to-periodic and periodic-to-periodic connections,” *BIT Numerical Mathematics*, **44**, 41–62.
- [Doedel and Friedman, 1989] E. J. Doedel and M. J. Friedman, [1989], “Numerical computation of heteroclinic orbits,” *J. Comput. Appl. Math.*, **26**, 155–170.
- [Doedel *et al.*, 1994] E. J. Doedel, M. J. Friedman, and A. C. Monteiro, [1994], “On locating connecting orbits,” *Appl. Math. Comput.*, **65**, 231–239.
- [Doedel *et al.*, 1997] E. J. Doedel, A. R. Champneys, T. F. Fairgrieve, Yu. A. Kuznetsov, B. Sandstede, and X. Wang, [1997], “AUTO97: Continuation and bifurcation software for ordinary differential equations.”, Technical report, Concordia University, Montreal, Quebec, Canada.
- [Freire *et al.*, 1993] E. Freire, A. J. Rodríguez-Luis, E. Gamero, and E. Ponce, [1993], “A case study for homoclinic chaos in an autonomous electronic circuit. A trip from Takens-Bogdanov to Hopf-šil’nikov,” *Phys. D*, **62**, 230–253.
- [Hogeweg and Hesper, 1978] P. Hogeweg and B. Hesper, [1978], “Interactive instruction on population interactions,” *Computational Biology and Medicine*, **8**, 319–327.
- [Klebanoff and Hastings, 1994] A. Klebanoff and A. Hastings, [1994], “Chaos in three-species food chains,” *J. Math. Biol.*, **32**, 427–451.
- [Kuznetsov and Levitin, 1997] Yu. A. Kuznetsov and V. V. Levitin, [1997], “CONTENT: Integrated environment for the analysis of dynamical systems.”. Centrum voor Wiskunde en Informatica (CWI), Kruislaan 413, 1098 SJ Amsterdam, The Netherlands. Available for download at <ftp://ftp.cwi.nl/pub/content>.
- [Kuznetsov and Rinaldi, 1996] Yu. A. Kuznetsov and S. Rinaldi, [1996], “Remarks on food chain dynamics,” *Math. Biosci.*, **134**, 1–33.

- [Kuznetsov *et al.*, 2001] Yu. A. Kuznetsov, O. De Feo, and S. Rinaldi, [2001], “Belyakov homoclinic bifurcations in a tritrophic food chain model,” *SIAM J. Appl. Math.*, **62**, 462–487.
- [McCann and Yodzis, 1995] K. McCann and P. Yodzis, [1995], “Bifurcation structure of a three-species food chain model,” *Theor. Pop. Biol.*, **48**, 93–125.
- [Pampel, 2001] T. Pampel, [2001], “Numerical approximation of connecting orbits with asymptotic rate,” *Numer. Math.*, **90**, 309–348.
- [Rosenzweig and MacArthur, 1963] M. L. Rosenzweig and R. H. MacArthur, [1963], “Graphical representation and stability conditions of predator-prey interactions,” *Am. Nat.*, **97**, 209–223.

## A Monodromy matrices

In order to approximate the invariant manifolds of a limit cycle we use eigenvalues and eigenfunctions of appropriate variational problems. These eigenvalues in turn are the eigenvalues of the so-called *monodromy matrix*.

To define an eigenfunction of the periodic solution  $x(t+T) = x(t)$ , where  $T$  is the period of the cycle, of an autonomous system of smooth ODE's

$$\dot{u} = f(u), \quad f : \mathbb{R}^n \rightarrow \mathbb{R}^n, \quad (33)$$

write a solution of this system near the cycle in the form

$$u(t) = x(t) + \xi(t),$$

where  $\xi(t)$  is a small deviation from the periodic solution. After substitution and truncation of the  $O(\|\xi\|^2)$ -terms, we obtain the following *variational system*:

$$\dot{\xi} = A(t)\xi, \quad \xi \in \mathbb{R}^n, \quad (34)$$

where  $A(t) = f_u(x(t))$  is the Jacobian matrix evaluated along the periodic solution;  $A(t+T) = A(t)$ .

Now, consider the matrix initial-value problem

$$\dot{Y} = A(t)Y, \quad Y(0) = I_n, \quad (35)$$

where  $I_n$  is the unit  $n \times n$  matrix. Its solution  $Y(t)$  at  $t = T$  is the *monodromy matrix* of the cycle:

$$M = Y(T).$$

The monodromy matrix is nonsingular. Any solution  $\xi(t)$  to (34) satisfies

$$\xi(T) = M\xi(0). \quad (36)$$

The eigenvalues of the monodromy matrix  $M$  are called the *Floquet multipliers* of the cycle. There is always a multiplier +1. Moreover, the product of all multipliers is positive:

$$\mu_1 \mu_2 \cdots \mu_n = \exp \left( \int_0^T \operatorname{div} f(x(t)) dt \right).$$

Together with (34), consider the *adjoint variational system*

$$\dot{\zeta} = -A^T(t)\zeta, \quad \zeta \in \mathbb{R}^n \quad (37)$$

and the corresponding matrix initial-value problem

$$\dot{Z} = -A^T(t)Z, \quad Z(0) = I_n, \quad (38)$$

which is the adjoint system to (35). Note, that the multipliers of the adjoint monodromy matrix

$$N = Z(T)$$

are the *inverse* multipliers of the monodromy matrix  $M = Y(T)$ . The proof of this well-known fact goes as follows. Compute

$$\begin{aligned} \frac{d}{dt}(Z^T Y) &= \frac{dZ^T}{dt} Y + Z^T \frac{dY}{dt} \\ &= (-A^T Z)^T Y + Z^T A Y \\ &= Z^T (-A) Y + Z^T A Y = 0. \end{aligned}$$

Since  $Z(0) = Y(0) = I_n$ , we get  $Z^T(T)Y(T) = I_n$ , which implies

$$N = [M^{-1}]^T.$$

Due to (36), a multiplier  $\mu$  satisfies  $v(T) = \mu v(0)$  with  $v(0) \neq 0$  or, equivalently, it is a solution component of the following BVP on the unit interval  $[0, 1]$ :

$$\begin{cases} \dot{v} + TA(t)v = 0, \\ v(1) - \mu v(0) = 0, \\ \langle v(0), v(0) \rangle - 1 = 0. \end{cases} \quad (39)$$

First assume that  $\mu > 0$  and write

$$\mu = e^\lambda, \quad v(t) = e^{\lambda t} w(t).$$

Then  $w$  satisfies a periodic BVP, namely:

$$\begin{cases} \dot{w} + TA(t)w + \lambda w = 0, \\ w(1) - w(0) = 0, \\ \langle w(0), w(0) \rangle - 1 = 0. \end{cases} \quad (40)$$

Similarly, when  $\mu < 0$ , we can introduce

$$\mu = -e^\lambda, \quad v(t) = e^{\lambda t} w(t)$$

and obtain an anti-periodic BVP

$$\begin{cases} \dot{w} + TA(t)w + \lambda w &= 0, \\ w(1) + w(0) &= 0, \\ \langle w(0), w(0) \rangle - 1 &= 0. \end{cases} \quad (41)$$

This technique can easily be adapted to the multipliers of the adjoint variational problem (37).

Finally, we note that the eigenvalue problem for a Floquet multiplier

$$Mv - \mu v = 0$$

can be considered as a *continuation problem* with  $n+1$  variables  $(v, \mu) \in \mathbb{R}^n \times \mathbb{R}$  defined by  $n$  equations. This continuation problem has a trivial solution family  $(v, \mu) = (0, \mu)$ . An eigenvalue  $\mu_1$  corresponds to a *branch point*, from which a *secondary solution family*  $(v, \mu_1)$  with  $v \neq 0$  emanates. This nontrivial family can be continued using an extended continuation problem

$$\begin{cases} Mv - \mu v &= 0, \\ \langle v, v \rangle - h &= 0, \end{cases}$$

which consists of  $n+1$  equation with  $n+2$  variables  $(v, \mu, h)$ . If  $h = 1$  is reached, we get a normalized eigenvector  $v$  corresponding to the eigenvalue  $\mu_1$ , since along this branch  $\mu \equiv \mu_1$ . Generalization of this procedure to the BVP (39) (as well as to (40), (41), and their adjoint versions) is straightforward.